Structures 29 (2021) 823–842

Contents lists available at ScienceDirect

Structures

journal homepage: www.elsevier.com/locate/structures

Experimental investigation and pseudoelastic truss model for in-plane behavior of corrugated sandwich panels with polyurethane foam core

Ercan Yüksel [a,*,1], Ahmet Güllü [b,2], Hasan Özkaynak [c,3], Cihan Soydan [d,4], Arastoo Khajehdehi [e,5], Erkan Şenol [e,6], Amir Mahdi Saghayesh [e], Hakan Saruhan [f]

[a] Faculty of Civil Engineering, Istanbul Technical University, Maslak, Istanbul, Turkey
[b] Department of Civil Engineering, Istanbul Gedik University, Kartal, Istanbul, Turkey
[c] Department of Civil Engineering, Beykent University, Maslak, Istanbul, Turkey
[d] Department of Civil Engineering, Namık Kemal University, Tekirdağ, Turkey
[e] Institute for Science and Technology, Istanbul Technical University, Maslak, Istanbul, Turkey
[f] Faculty of Civil Engineering, Istanbul Technical University, Maslak, Istanbul, Turkey

ARTICLE INFO

Keywords:
Sandwich panels
Analytical modelling
Mechanical properties
Mechanical testing

ABSTRACT

Sandwich panels are commonly used in façades and the roofs of industrial buildings due to their well-known advantages. However, there is limited data about the in-plane behavior of the panels. Hence, this paper aimed to propose a pseudoelastic truss model to represent the effective in-plane stiffness and strength properties of the corrugated sandwich panels with a polyurethane foam core. Two separate sets of experiments (mock-up and system test) were conducted in the laboratory. The variables were the number of fasteners, sheet thickness, loading direction, and number of ribs. The number of fasteners, sheet thickness, and loading direction are the most effective parameters for the in-plane behavior. A formula was proposed to compute axial stiffness of the truss members by considering the effective parameters. Experimental results showed that the proposed robust truss model could give a good estimate of the pseudoelastic stiffness and maximum load bearing capacity of the sandwich panels.

1. Introduction

Sandwich panels have a wide range of application area due to their advantages such as insulation, high strength-to-self weight ratio, fast construction time, high corrosion resistance, re-useability long spanning capability, etc. Because of the slender structure of sandwich panels, their contribution to the overall structural response are mostly neglected during traditional design. However, modern design approaches such as Turkish Building Seismic Code (*TBSC*) 2018 [1] and CIB [2] require the consideration of sandwich panels in the description of diaphragm action in the roof plan. In this circumstance, the main goals of this paper are to assess the in-plane behavior of corrugated sandwich panels with polyurethan foam core and to propose a reliable numerical pseudoelastic truss model.

Mahfuz et al. [3] experimentally investigated buckling of sandwich panels considering the effects of core-skin debonding and core density. Their study showed that the core density has a significant effect on the global buckling. Dariushi and Sadighi [4] investigated the flexural performance of sandwich panels having fiber metal laminate faces. That study was performed on six groups of specimens and showed that fiber metal laminate faces have reasonable resistance to transverse local loads. Mostafa et al. [5] investigated the shear response of the composite sandwich panels with polyvinylchloride (*PVC*) foam core and glass fiber reinforced polymer (*GFRP*) skins. The experiments indicated that

* Corresponding author.
E-mail address: yukselerc@itu.edu.tr (E. Yüksel).
[1] ORICD: 0000-0002-9741-1206.
[2] ORICD: 0000-0001-6678-9372.
[3] ORICD: 0000-0003-2880-7669.
[4] ORICD: 0000-0003-3579-0033.
[5] ORICD: 0000-0003-3357-2251.
[6] ORICD: 0000-0002-3290-945X.

https://doi.org/10.1016/j.istruc.2020.11.058
Received 25 January 2020; Received in revised form 29 October 2020; Accepted 20 November 2020
Available online 15 December 2020

a) The specimens with two ribs b) The specimens with four ribs

Fig. 1. The corrugated sandwich panels.

Table 1
Monotonic tension tests.

# Test	# of ribs	Total sheet thickness (mm)	Loading direction against ribs	# of fasteners
1	4	0.9	Parallel	14
2	4	0.9		7
3	2	0.9		14
4	2	0.9		7
5	4	0.9	Perpendicular	14
6	4	0.9		7
7	2	0.9		14
8	2	0.9		7
9	4	1.7	Parallel	14
10	4	1.7		7
11	4	1.7	Perpendicular	14
12	4	1.7		7

dominant failure mode was skin-core debonding. Mostafa et al. [6] investigated flexural behavior and failure mode of composite sandwich panels through four-point bending tests. The dominant failure mode was found to be core shear failure associate with skin-core debonding close to the loading point. Avci et al. [7] carried out full-scale tests and analytical studies on corrugated aluminum roof panels. The experimentally and analytically obtained shear strength and stiffness properties agreed with each other. A modified panel edge term ($k = 2/3$) was proposed to calculate shear stiffness of the aluminum panel diaphragms. Yu et al. [8] derived implicit equations to determine the elastic properties of adhesively bonded corrugated core sandwich panels. Three-dimensional finite element analyses were conducted on the simply supported sandwich panel to verify the validity of the derived equation and elastic constants. The analyses consisted of 3D FEM analyses results. Qi and Ma [9] performed pull-out and shear tests on composite pyramidal truss core sandwich panels with lightweight metallic quadrangular-prism inserts. The experimental results showed that the designed panels have similar pull-out strength with honeycomb panels while its shear capacity was larger. Sarvestani et al. [10] performed numerical and experimental studies on 3D printed light-weight sandwich panels with architected cellular cores under low-velocity impact. Diverse types of cell topologies were generated by changing the geometrical parameters. The results showed that the auxetic sandwich panel was the best for energy absorption. Daliri and Zeinedini [11] developed bidirectional sinusoidally corrugated core sandwich panel. The core patterns of the test specimens were in different forms. They concluded that the specimen with the core period of 37.5 mm has the best energy absorption.

Although there are many studies on the out-of-plane behavior of sandwich panels, there are a limited number of studies for in-plane behavior. De Matteis and Landolfo [12] performed monotonic and cyclic full-scale shear tests on å single specimen and integrated panels under lateral loads. The cyclic experiments showed that the specimens have low energy dissipative capacity due to large hole elongations that occurred at fastener locations. Dependently, improvements in the current fastening system were suggested. Mahendran and Subaaharan [13] conducted experiments to investigate the shear behavior of sandwich panel systems with crest-fixing. The experiments indicated that the current fastening practice was inappropriate to benefit full shear capacity due to the brittle failure of fasteners. The proposed improved fastening system considerably increased the overall strength and initial stiffness. Rogers and Tremblay [14] conducted experiments to investigate the inelastic seismic response of metal deck roofing systems with different connection conditions. Powder-actuated fastener connections could provide the highest energy dissipation where welded connections exhibited significant ultimate capacities with small displacements resulting in low energy dissipation. Essa et al. [15] carried out large scale monotonic and quasi-static cyclic experiments on corrugated cold-formed steel deck diaphragms with different fastening details. The test results indicated that diaphragms with welded deck-to-frame fasteners without washers have limited ductility. However, using mechanical and welded deck-to-frame fasteners resulted in enhanced strength and ductility.

Peirick and Dawood [16] tested glass fiber reinforced polymer (*GFRP*) sandwich panels subjected to in-plane biaxial loading. The experiments used different configurations and suggested that the in-plane behavior of the panels mainly depends on their out-of-plane stiffness. Massarelli et al. [17] conducted a series of in-plane dynamic tests on steel deck roof diaphragm along two orthogonal directions. They concluded that ductility of the decks is reduced by using thicker specimen and parallel loading conditions. Hamid and Fudzee [18] conducted experiments to evaluate the seismic performance of insulated sandwich panels under in-plane lateral cyclic loading. Experimental observations displayed that the cracks were initiated through wall-to-foundation joints and buckling of aluminum panel. Choi et al. [19] performed push-out tests to investigate in-plane shear performance of concrete sandwich panels having diverse insulation material with and without corrugated shear connectors. They found that type of the insulation material considerably affected bond strength between the concrete walls and the insulation layer. Motamedi and Ventura [20] conducted in-plane shear tests on steel roof deck diaphragms. The test program was designed to evaluate the seismic inelastic response of steel roof decks with different thicknesses and different types of deck-to-frame connections. Test results exposed that inelastic deformation was concentrated on the edge of the diaphragms and parallel to the lateral loading. The post peak behavior of welded specimens resulted in significant deterioration and rapid strength reduction.

Sandwich panels with polyurethane foam core are stabilizing

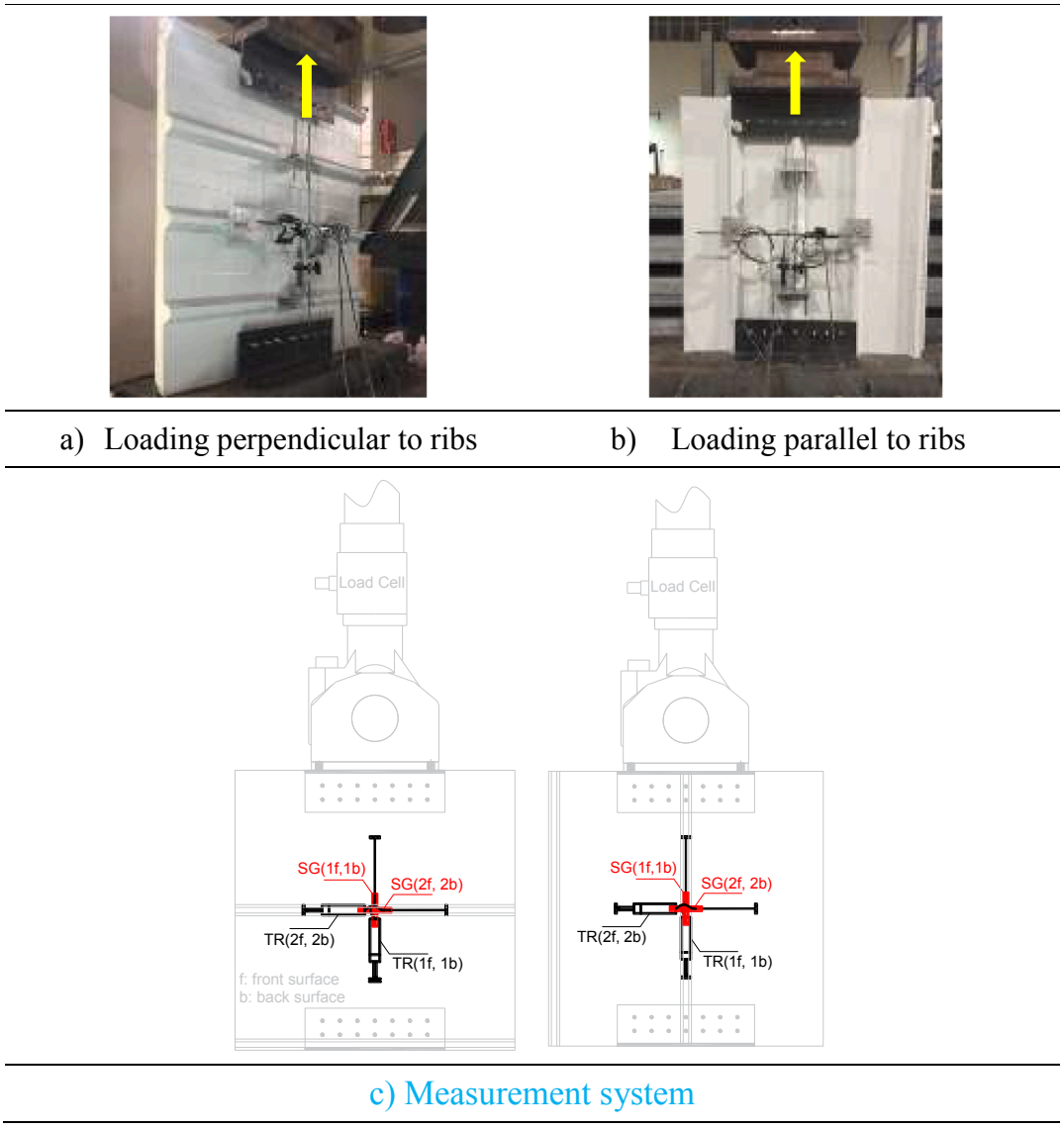

Fig. 2. Set-up for mockup tests.

elements for sole steel members such as beam, column, and purlin [2]. Sandwich panels provide stiffness against displacements in their own plane, improve the torsional rigidity, and prevent buckling of the supporting structural members. The stabilization capability requires one to have exact knowledge about the in-plane shear stiffness of sandwich panels. Special attention should also be paid to the design of fastenings. Moreover, *TBSC* [1] enforces the designers to include the sandwich panels at the roof into the numerical models of the precast structural systems.

Flexural, shear, buckling, as well as in-plane characteristics of the sandwich panels having assorted properties such as sheet and core materials and core type have been studied individually in the literature. However, there is little information about all of these behavioral parameters affecting the in-plane behavior of corrugated sandwich panes with a polyurethane foam core. Therefore, a comprehensive experimental campaign was conducted on the subject. The rationale of this paper is to propose an *effective stiffness formula* for the pseudoelastic truss model to represent in-plane behavior of the sandwich panels.

2. The experimental study

The experimental work consists of two parts: *monotonic mockup tests* and *cyclic system tests*, Saghayesh [21].

The sandwich panel consists of a corrugated face, polyurethane foam core, and a flat face. The rib numbers were two and four (Fig. 1). Corrugated and flat faces were made up steel sheets having thicknesses of 0.4 mm and 0.5 mm; 1.0 mm and 0.7 mm for two independent groups of specimens. The dimensions of the mockup were 1000 mm (w) × 1000 mm (h) × 75 mm (t).

Average yielding strength and strain derived from the performed

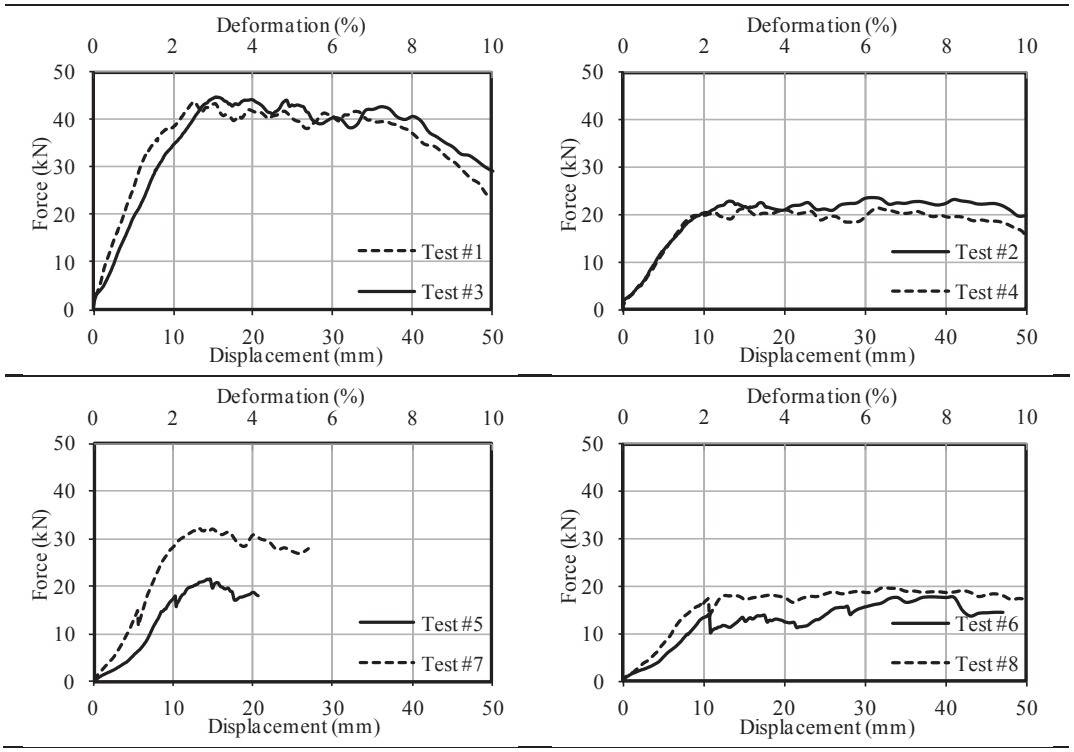

Fig. 3. Rib effect on the behavior.

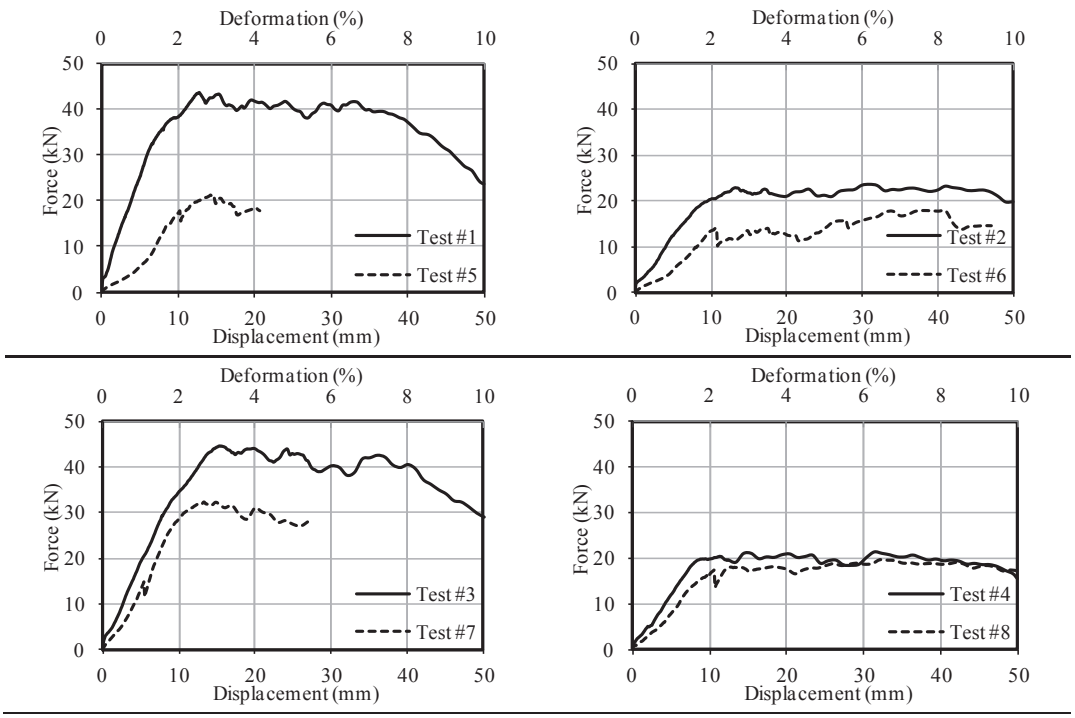

Fig. 4. Loading direction effect on the behavior.

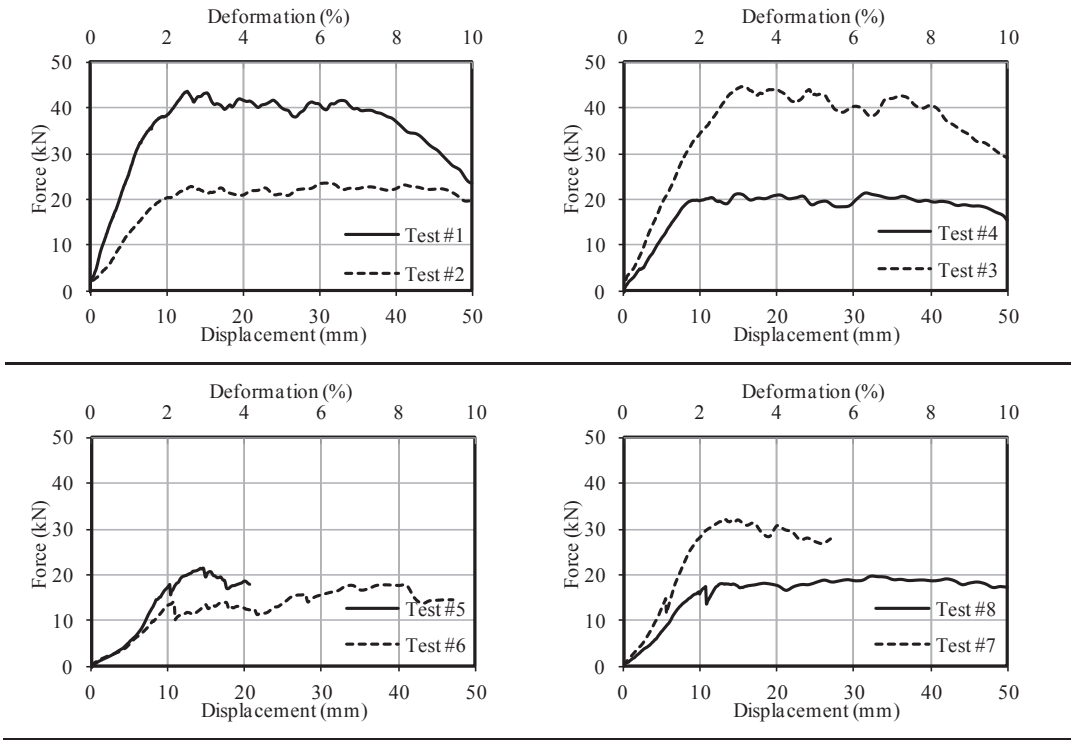

Fig. 5. Fastener effect on the behavior.

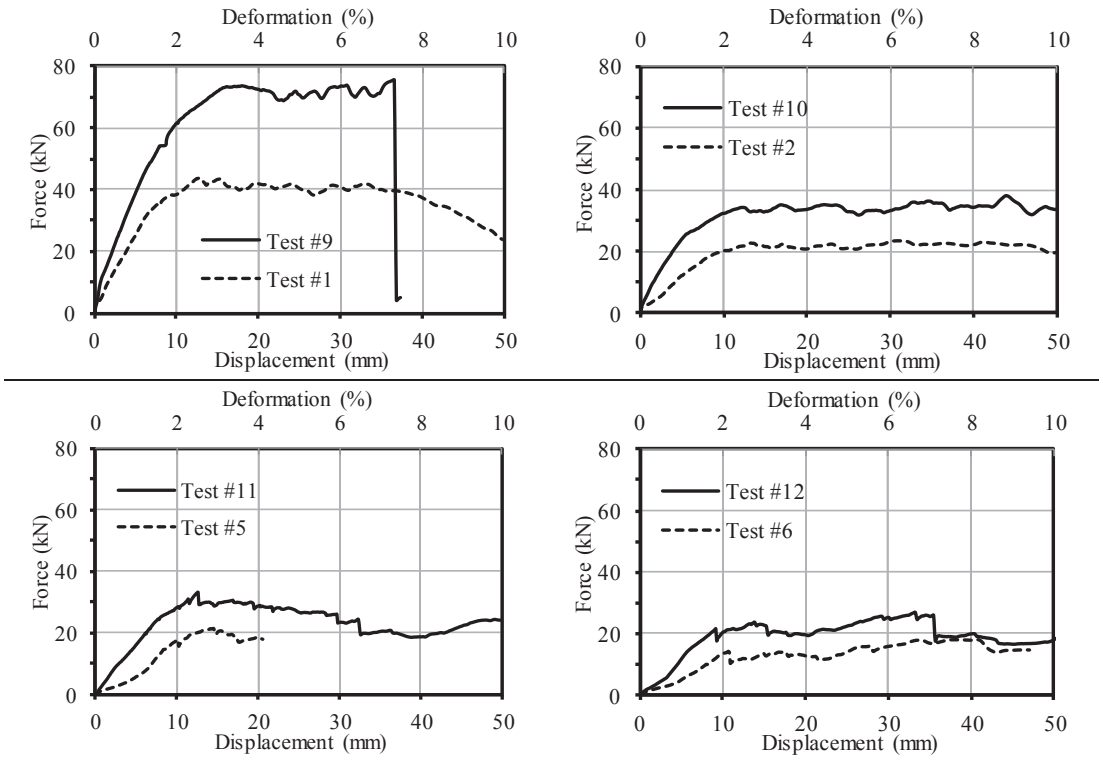

Fig. 6. Sheet thickness effect on the behavior.

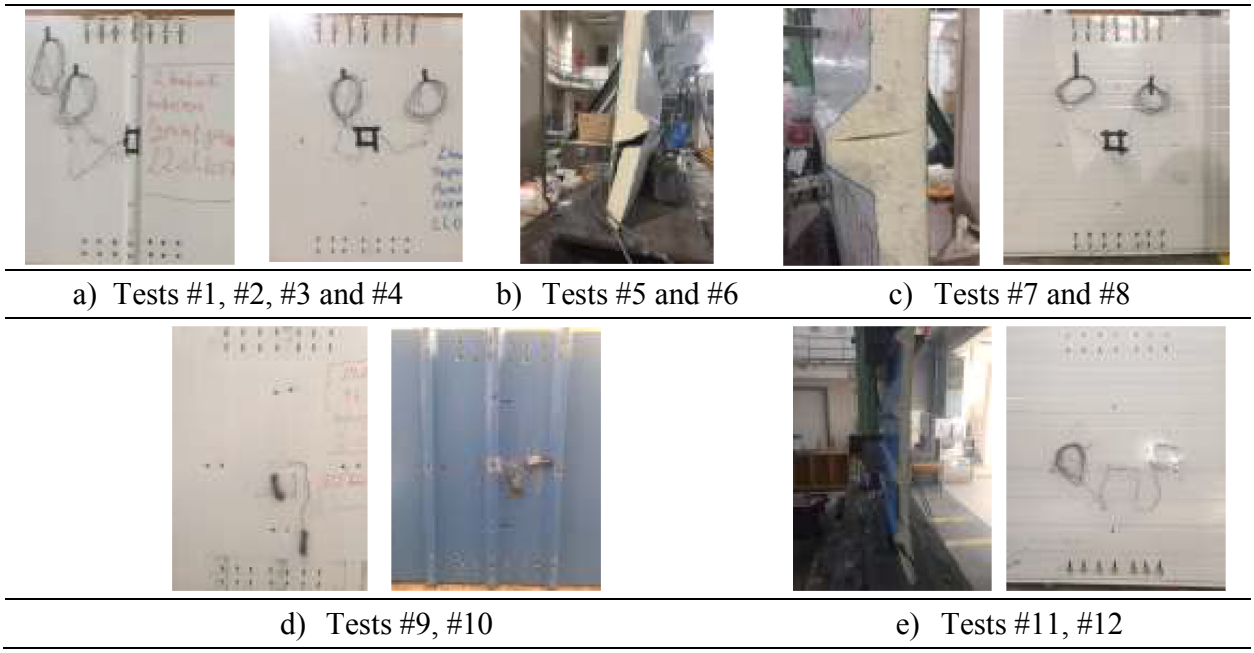

Fig. 7. Damage observed in the mockup tests.

Table 2
Modulus of elasticity (MPa) for thinner specimens loaded parallel to the ribs.

Approach	Corrugated Face				Flat Face			
	Test#1	Test#2	Test#3	Test#4	Test#1	Test#2	Test#3	Test#4
# 1	103,067	58,854	115,434	59,871	85,051	90,736	82,388	121,031
# 2	98,171	47,583	95,436	53,648	88,449	91,627	87,771	149,695
# 3	102,080	57,828	116,300	59,264	85,067	88,759	81,020	129,645
Average	101,106	54,755	109,056	57,594	86,189	90,374	83,726	133,457
Overall Average	89,532							

coupon tests for the 0.5 mm thick flat sheet were 255 MPa and 0.26%, respectively.

2.1. Mockup tests

Twelve monotonic tension tests were performed on discrete mock-ups. The variables were number of ribs, the loading direction, and the number of fasteners. A summary of the test configuration is given in Table 1.

A servo-controlled MTS actuator was utilized in the tests (Fig. 2a, b). The specimens were attached to the actuator and the supporting frame via the brackets. Several measurements were taken from various locations of the specimens during the tests. Two sets of strain gauges and transducers were placed orthogonally at the center to measure the strains and displacements at both faces, Fig. 2c.

The force displacement curves are demonstrated in Figs. 3–5 to assess the effects of the selected variables. The responses are discussed broadly in the succeeding paragraphs.

2.1.1. The effect of rib numbers

Responses of the specimens having identical number of fasteners and loading directions are compared in Fig. 3. Yielding forces obtained from tests #1 and #3 are 44 kN and 45 kN, respectively. Whereas yielding forces reached in tests #2 and #4 are 23 kN and 21 kN respectively. For the cases of specific number of fasteners and the loading in parallel direction, the load-bearing capacity was not significantly affected by the rib numbers. However, yielding forces obtained from tests #5 and #7 are 18 kN and 32 kN whereas 11 kN and 18 kN for tests #6 and #8. The specimens tested in perpendicular direction suggest that the load-bearing capacity increases almost 60% to 75% if the number of ribs increases twice.

2.1.2. The effect of loading direction

Responses of the specimens having an identical number of fasteners and ribs are compared with each other to evaluate the effect of the loading direction (Fig. 4). Yielding forces obtained from tests #1 and #5 are 44 kN and 18 kN, respectively. The yielding forces reached from tests #2 and #6 are 23 kN and 11 kN. Tensile strength of the specimens having four ribs with a specific number of fasteners increased almost double as loading direction shifted from perpendicular to parallel.

The yielding forces obtained from tests #3 and #7 are 45 kN and 32 kN, respectively. Whereas, the yield force derived from tests #4 and #8 are 21 kN and 18 kN. For an identical number of ribs, the yield force increased almost 44% and 35% as the loading direction changed from perpendicular to parallel for the specimens with fastener numbers of 14 and 7, respectively.

Table 3
Modulus of elasticity (MPa) for thinner specimens loaded perpendicular to the ribs.

Approach	Corrugated Face				Flat Face			
	Test#5	Test#6	Test#7	Test#8	Test#5	Test#6	Test#7	Test#8
# 1	53,090	58,625	64,827	45,582	74,891	122,439	102,878	*N.A.*
# 2	51,043	57,617	64,061	45,400	77,788	120,474	102,352	*N.A.*
# 3	60,917	57,081	67,737	45,190	73,742	129,861	105,088	*N.A.*
Average	55,017	57,774	65,542	45,391	75,474	124,258	103,439	*N.A.*
Overall Average	78,494							

Table 4
Modulus of elasticity (MPa) for thicker specimens.

Approach	Corrugated Face		Flat Face		Corrugated Face		Flat Face	
	Test#9	Test#10	Test#9	Test#10	Test#11	Test#12	Test#11	Test#12
# 1	45,447	46,079	174,948	67,631	61,219	35,801	137,368	60,697
# 2	54,700	47,393	178,646	77,745	61,651	22,440	172,934	48,292
# 3	56,330	46,451	162,183	76,673	59,973	25,596	244,335	50,016
Average	52,159	46,641	171,926	74,016	60,948	27,946	184,879	53,001
Overall Average	86,186				81,694			

Table 5
Description of the system tests.

Group #	Test #	Loading irection	Number of ribs	Arrangement of Fasteners
First	1	Perpendicular	2	1-1-1-1-1
	2		2	2-2-3-2-2
	3		4	2-2-3-2-2
Second	4	Parallel	4	2-2-3-2-2
	5		2	2-2-3-2-2
	6		4	1-1-1-1-1

2.1.3. The effect of fastener numbers

The specimens having identical number of ribs and loading direction are compared to recognize the effect of fastener numbers (Fig. 5). The yielding forces obtained from tests #1 and #2 are 44 kN and 23 kN, respectively. The yielding forces reached in tests #3 and #4 are 45 kN and 21 kN. In the case of parallel loading, the increment ratio in yielding forces are derived as 1.91 (=44/23) and 2.14 (=45/21) if the number of the fasteners are doubled. Alternatively, yielding forces obtained from tests #5 and #6 are 18 kN and 11 kN. The yielding realized in tests #7 and #8 are 32 kN and 18 kN. It increased about 1.64- and 1.78-times as the fasteners doubled. The yielding force increases as the number of fasteners becomes independent from the loading direction.

2.1.4. The effect of sheet thickness

The response of the specimens having identical numbers of ribs and fasteners were compared to recognize the effect of total sheet thickness for two loading directions (Fig. 6). Yielding forces obtained from tests #1 and #9 are 44 kN and 73 kN, respectively. The yielding forces reached in tests #2 and #10 are 23 kN and 34 kN. In the case of parallel loading, the increment ratios are realized as 1.66 and 1.48. Yielding forces obtained from tests #5 and #11 are 18 kN and 33 kN, respectively. The yielding forces reached in tests #6 and #12 are 11 kN and 22 kN, respectively. The ratios are determined as 1.83 and 2.00 for the perpendicular loading. The experiments showed that the increase in sheet thickness provided 60% and 90% increments in yielding forces.

2.1.5. Damage observations

The typical damage patterns are presented in Fig. 7.

The common failure mode observed in tests #1 to #4 were yielding and shearing of sheets around fasteners (Fig. 7a). The failure mechanism for tests #5 and #6 was breaking of the polyurethane core and debonding of the flat sheets (Fig. 7b). In tests #7 and #8; yielding and shearing of sheets around the fasteners were observed at both faces but there was no debonding of the sheets (Fig. 7c). The failure mode observed in tests #9 to #12 showed shearing of sheets around fasteners (Fig. 7d). Breaking of the polyurethane core was also observed in tests #11 and #12 (Fig. 7e). Leading failure mode was determined to be yielding and shearing around the fasteners for the specimens excited to the parallel loading. However, for perpendicular loading, the load is transferred indirectly over the corrugated surfaces and thus the failure mode turned out to be the skin-core debonding.

2.2. Calculation of equivalent modulus of elasticity

The modulus of elasticity was determined from the experimentally obtained stress–strain relations. The actuator force is dispersed between corrugated and flat faces proportional with their sectional areas. The axial stress was calculated by dividing the sheet force to its sectional area. The strain was measured directly by strain gauges.

Three discrete approaches were utilized in the determination of modulus of elasticity:

1- Slope of the trend line generated for ascending the branch of the curve until yielding stress (σ_y).
2- Slope of the trend line generated for the curve between 5% and 35% of σ_y.
3- Slope of the line connecting the origin to the point of $\sigma_y/3$.

The modulus of elasticities calculated by three approaches are listed in Tables 2–4.

The modulus of elasticity is discreetly affected by the numbers of ribs and fasteners as well as sheet thickness. The results are compiled with respect to sheet thickness of the specimens.

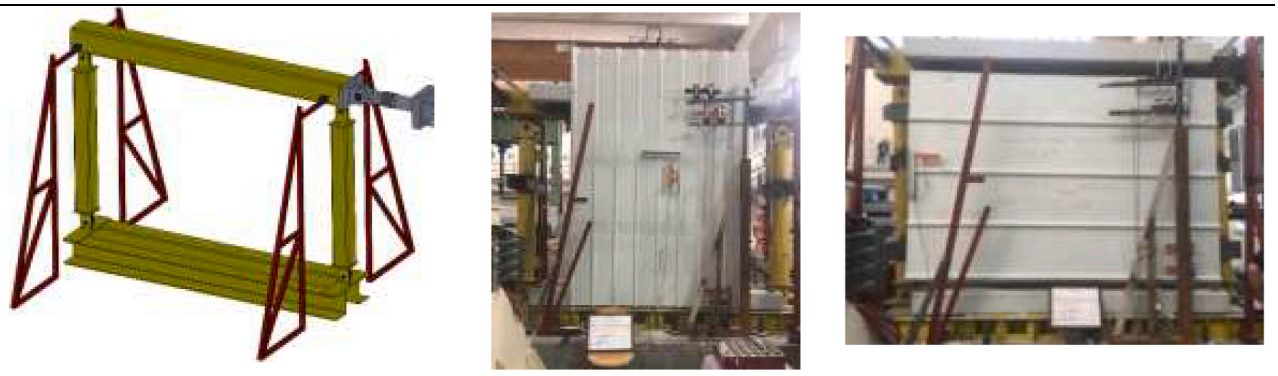

a) Four pinned testing frame b) Perpendicular Loading c) Parallel Loading

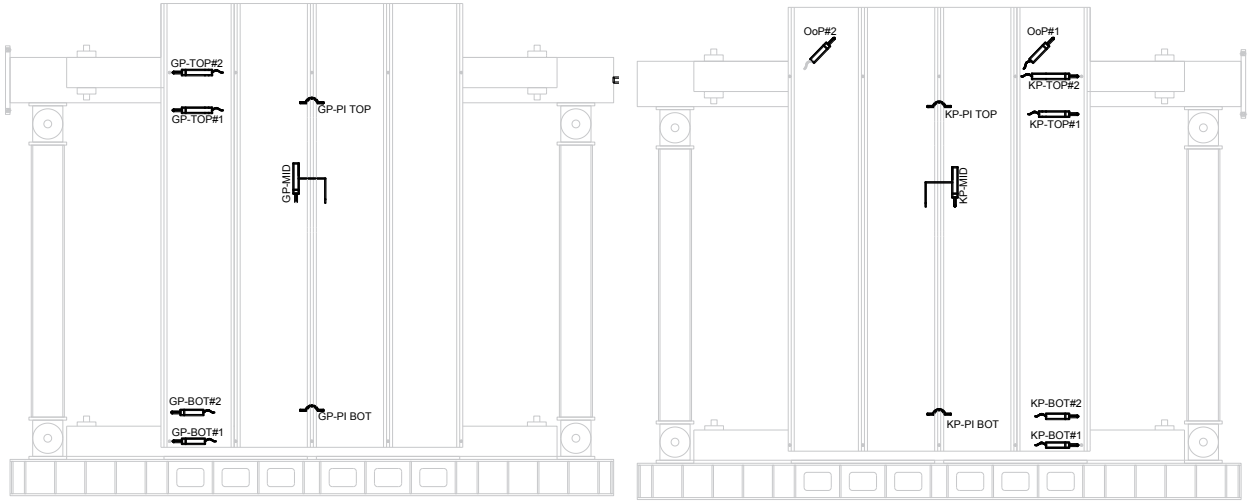

d) Measurement system for perpendicular loading

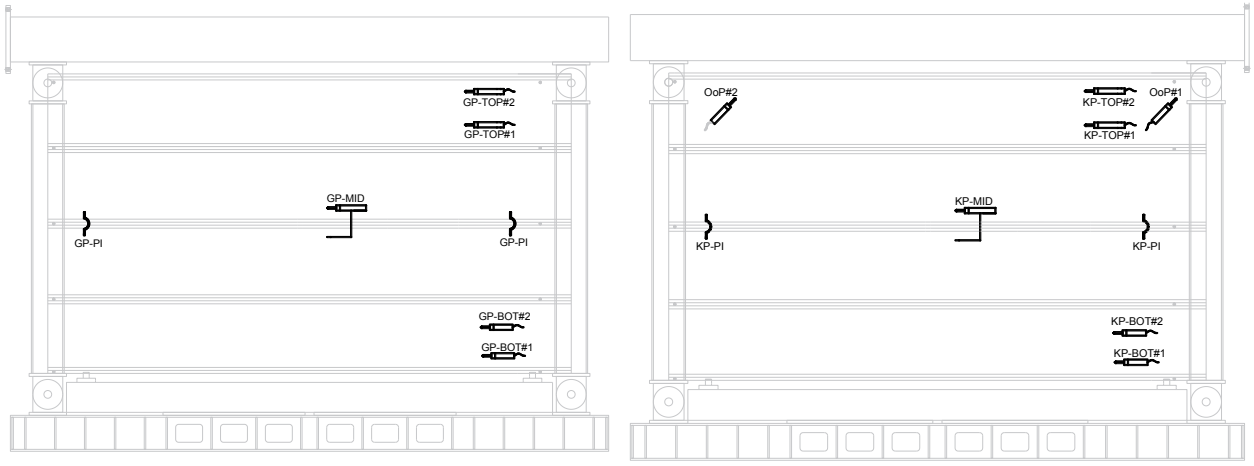

e) Measurement system for parallel loading

Fig. 8. Testing set-up for the system tests.

a) Chest Fixing b) Valley Fixing

Fig. 9. Typical fastener arrangements.

Table 6
The displacement pattern utilized in the system tests (FEMA 461, 2007).

Step #	1	2	3	4	5	6	7	8	9	10	11
a_i/a_{10}	0.018	0.025	0.035	0.048	0.068	0.095	0.133	0.186	0.260	0.364	0.510
Displ. (mm)	5.40	7.55	10.58	14.29	20.95	28.28	40.64	55.75	78.98	109.64	154.64

- *Tests #1 to #8:* Modulus of elasticity for the parallel loading varied between 55,000 to 110000 MPa and 83,000 to 134000 MPa for corrugated and flat surfaces, respectively. The perpendicular loading deviates between 45,000 to 65000 MPa and 75,000 to 125000 MPa for corrugated and flat surfaces, respectively. The overall average is determined as 84000 MPa.
- *Tests #9 to #12:* In the parallel loading, the modulus of elasticity varied between 45,447 to 56330 MPa and 67,631 to 178646 MPa for corrugated and flat surfaces, respectively. It changes between 22,440 to 61651 MPa and 48,292 to 244335 MPa for corrugated and flat surfaces, respectively, in the perpendicular loading. The overall average is about 84000 MPa.

The Poisson ratio was 0.19–0.33 from the strain gauge measurements.

2.3. System tests

Six full-scale system tests were carried out by using reversal cyclic loading. The main parameters were number of ribs, loading direction, and fastener arrangement scheme. The experimental program is given in Table 5 in which the last column corresponds to numbers of fasteners on each rib.

Each test specimen consists of four panels. Two couples of panels in the dimensions of 2 × 3 m^2 were positioned at both sides of the four pinned steel testing frame. Out-of-plane movement of the test set-up is avoided by triangular truss-type restrictors on both sides (Fig. 8a). The panels were fixed to reinforced concrete purlins that were attached to the steel frame by the fasteners. Span length of the sandwich panels was 2.4 m and 2.0 m for the loadings perpendicular and parallel to ribs, respectively. The components of the testing set-up are given in Fig. 8b, c. The measurement system is also illustrated in Fig. 8d, e.

Five points at both ends of the sandwich panels were fixed to the purlins. The screws were positioned at some chests with an overlapping area of the adjacent panels. Edge connections of the panels were made by valley fixing. Typical fastener arrangements are illustrated in Fig. 9.

Displacement reversals were applied by the horizontally oriented MTS actuator that were connected to the four pinned testing frame. Each displacement target was repeated two times, Table 6.

2.3.1. Experimental results

Lateral force vs. drift relations and typical damage photos of the first group of specimens are presented in Fig. 10. Drift was calculated by dividing the lateral displacement to span length of the panels.

The initially observed damage in test #1 was sheet tearing on the overlapping ribs. The holes enlarged with final failure of the fasteners. The test demonstrated that the number of fasteners at overlapping ribs should be increased to magnify the in-plane strength of the panel system. The strength of the panel system could be increased about three-fold when the fastener configuration was improved. In tests #2 and #3, number of fasteners were increased to 2 for ordinary ribs and 3 for the overlapped ribs. After that, the similar damage propagation was observed for tests #2 and #3. Moreover, local buckling of the sheet was observed at the overlapping ribs in test #2. This was probably associated with the uncontrolled fastener intervals. No buckling event was observed in test #3.

Lateral force vs. drift relations and typical damage photos of the second group of specimens are presented in Fig. 11. The observed damage patterns for tests #4, #5, and #6 were similar. The shear dominant response was governed by sheet tearing at the ribs. It was followed by hole elongation, fastener fracture, and relative sliding of panels. In the case of test #6, lower strength was observed because the

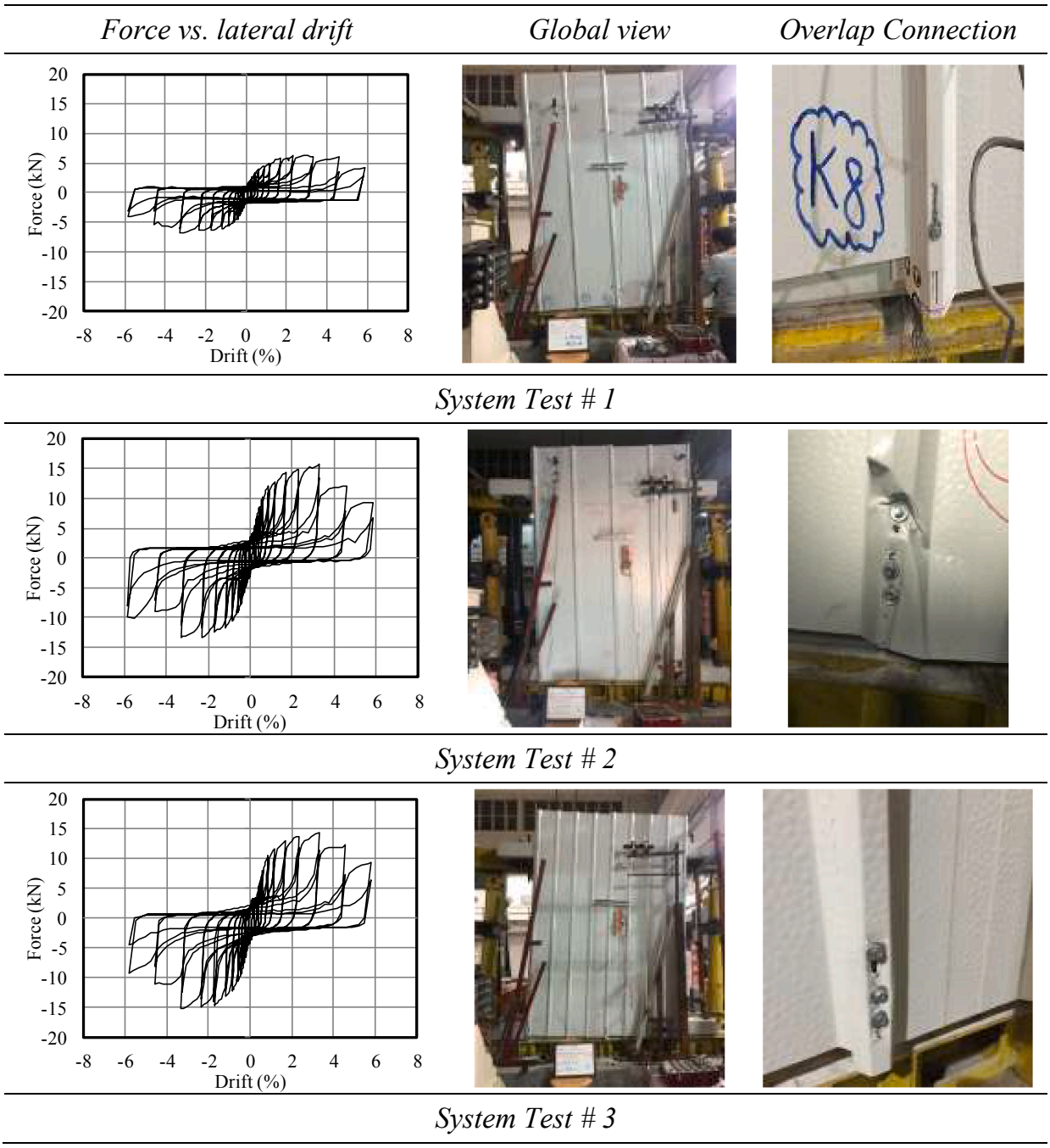

Fig. 10. Test results of the first group specimens.

fastener configuration was weaker than those of tests #4 and #5. Moreover, we concluded that the damage accumulation could be delayed if the fastener configuration is improved.

2.3.2. Evaluation of the test results in terms of in-plane stiffness

In-plane stiffness of the sandwich panel systems was determined in terms of *initial stiffness* (for 0.11% drift) and *the stiffness corresponding to ultimate drift*. Three diverse approaches namely *peak-to-peak*, *zero-to-peak,* and *three partite* were utilized in the calculations of these stiffnesses (Fig. 12 and Tables 7 and 8).

The responses of the specimens were not identical in the first and second cycles of the displacement targets. Because of the sheet tearing that arises in the first cycle of some displacement targets, the ultimate load as well as lateral stiffness decrease in the following cycle. The reductions were 75% to 95% especially at the larger displacement targets. The greatest stiffness reductions were observed in tests #1 and #6 where the weaker fastening conditions were utilized.

Since the global behavior of the sandwich panel system was governed by tearing of the sheets, three partite stiffness is advised to be a more reliable definition for the representation of the cyclic behavior.

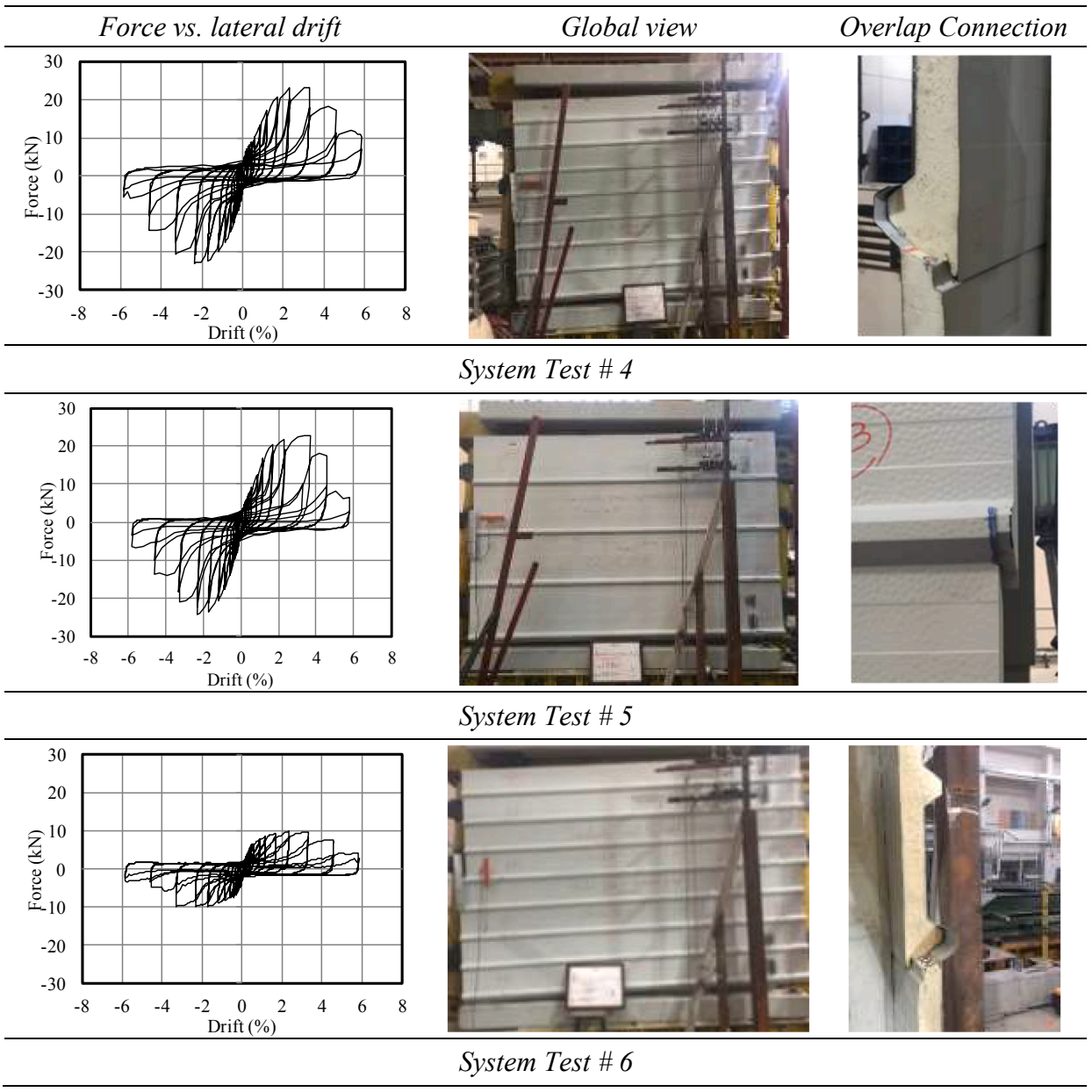

Fig. 11. Test results of the second group of specimens.

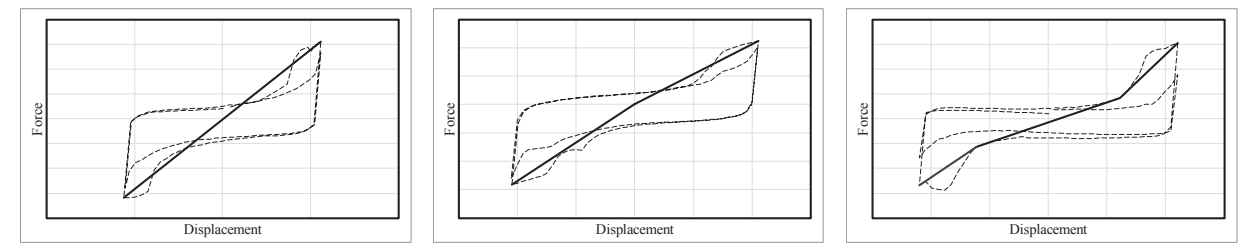

Fig. 12. Three diverse approaches utilized in calculation of the stiffnesses.

Table 7
In-plane stiffness comparison for the first group of specimens.

	Stiffness Determination Method		Initial Stiffness (kN/mm)		Stiffness @ max. drift (kN/mm)		Stiffness Reduction Ratio (%)	
			1st Cycle	2nd Cycle	1stCycle	2ndCycle	1stCycle	2ndCycle
Test # 1	Peak-to-peak (p-to-p) stiffness		0.71	0.72	0.03	0.02	95	97
	Zero to peak stiffness	Push (+)	0.56	0.58	0.03	0.02	94	96
		Pull (-)	0.84	0.86	0.03	0.02	97	98
	Three partite stiffness	Mid part	0.15	0.12	0.01	0.01	94	95
		Positive	0.22	0.71	0.07	0.07	68	90
		Negative	0.27	0.78	0.07	0.07	74	91
Test # 2	Peak-to-peak (p-to-p) stiffness		1.40	1.42	0.06	0.05	95	96
	Zero to peak stiffness	Push (+)	1.48	1.53	0.06	0.04	96	97
		Pull (-)	1.33	1.32	0.07	0.05	94	96
	Three partite stiffness	Mid part	0.37	0.38	0.02	0.01	94	96
		Positive	0.77	0.85	0.13	0.20	83	76
		Negative	0.68	0.96	0.12	0.15	82	84
Test # 3	Peak-to-peak (p-to-p) stiffness		1.41	1.42	0.06	0.03	96	98
	Zero to peak stiffness	Push (+)	1.13	1.15	0.06	0.04	95	96
		Pull (-)	1.70	1.68	0.06	0.03	96	98
	Three partite stiffness	Mid part	0.38	0.28	0.03	0.02	92	92
		Positive	0.73	0.91	0.15	0.13	79	85
		Negative	0.68	1.07	0.11	0.07	83	93

Table 8
In-plane stiffness comparison for the second group of specimens.

	Stiffness Determination Method		Initial Stiffness (kN/mm)		Stiffness @ max. drift (kN/mm)		Stiffness Reduction Ratio (%)	
			1st Cycle	2nd Cycle	1st Cycle	2nd Cycle	1st Cycle	2nd Cycle
Test # 4	Peak-to-peak (p-to-p) stiffness		2.26	2.22	0.06	0.04	97	98
	Zero to peak stiffness	Push (+)	1.93	1.90	0.07	0.05	96	97
		Pull (-)	2.57	2.53	0.04	0.03	98	99
	Three partite stiffness	Mid part	0.45	0.39	0.02	0.02	95	94
		Positive	0.83	1.36	0.12	0.10	85	92
		Negative	0.94	1.17	0.06	0.08	93	93
Test # 5	Peak-to-peak (p-to-p) stiffness		1.69	1.71	0.05	0.02	97	98
	Zero to peak stiffness	Push (+)	1.19	1.25	0.04	0.01	96	99
		Pull (-)	2.18	2.16	0.04	0.02	98	99
	Three partite stiffness	Mid part	0.52	0.41	0.02	0.01	96	97
		Positive	0.87	1.11	0.07	0.06	91	94
		Negative	0.81	0.99	0.06	0.05	92	95
Test # 6	Peak-to-peak (p-to-p) stiffness		1.17	1.22	0.02	0.01	98	99
	Zero to peak stiffness	Push (+)	0.60	0.62	0.03	0.02	95	96
		Pull (-)	1.78	1.74	0.02	0.01	98	99
	Three partite stiffness	Mid part	0.26	0.20	0.01	0.01	96	97
		Positive	0.34	0.36	0.05	0.06	85	83
		Negative	0.31	0.38	0.04	0.04	92	94

2.3.3. Evaluation of fastener effect

Specimens with identical number of ribs and loading direction were compared to assess the effect of fasteners on the global response. Lateral force vs. drift and lateral force vs. relative panel displacement relations for tests #1, #2 and #4, #6 are compared in Fig. 13. According to the graphics, we resolved that the in-plane stiffness and strength properties as well as post-peak behavior of sandwich panel system increased apparently by using more fasteners. These experimental observations resulted in a greater enclosed area of load vs. displacement cycles that were ensured by using better fastening conditions.

The comparison made for the secant stiffness is presented in Fig. 14 for the related specimens.

The stiffness values are bigger in test #2 and test #4 compared with their corresponding specimens. The graphics obviously display the effect of the fasteners on in-plane stiffness.

2.3.4. Evaluation of rib numbers

The specimens tested in identical loading direction with equal number of fasteners (tests #2, #3 and #4, #5) are compared to evaluate the rib effect (Fig. 15). We concluded that there is no significant effect of rib number on in-plane hysteretic behavior of the specimens.

There was no significant difference between the secant stiffness of the specimens (Fig. 16). The initial stiffness values are 1.41 and 1.42 kN/mm for test #2 and #3, respectively. The values are 2.26 and 1.69 kN/mm for tests #4 and #5, but this small difference disappeared after the 0.59% drift.

2.3.5. Evaluation of the loading direction

The specimens having identical fastener arrangements and equal number of ribs (tests #2, #5 and #3, #4) were compared to examine the effect of loading direction (Fig. 17). The ratio of the ultimate strengths of test #5 and test #2 is 1.43 and 1.61 for test #4 and test #3. The experimental results show that the in-plane load-bearing capacity is

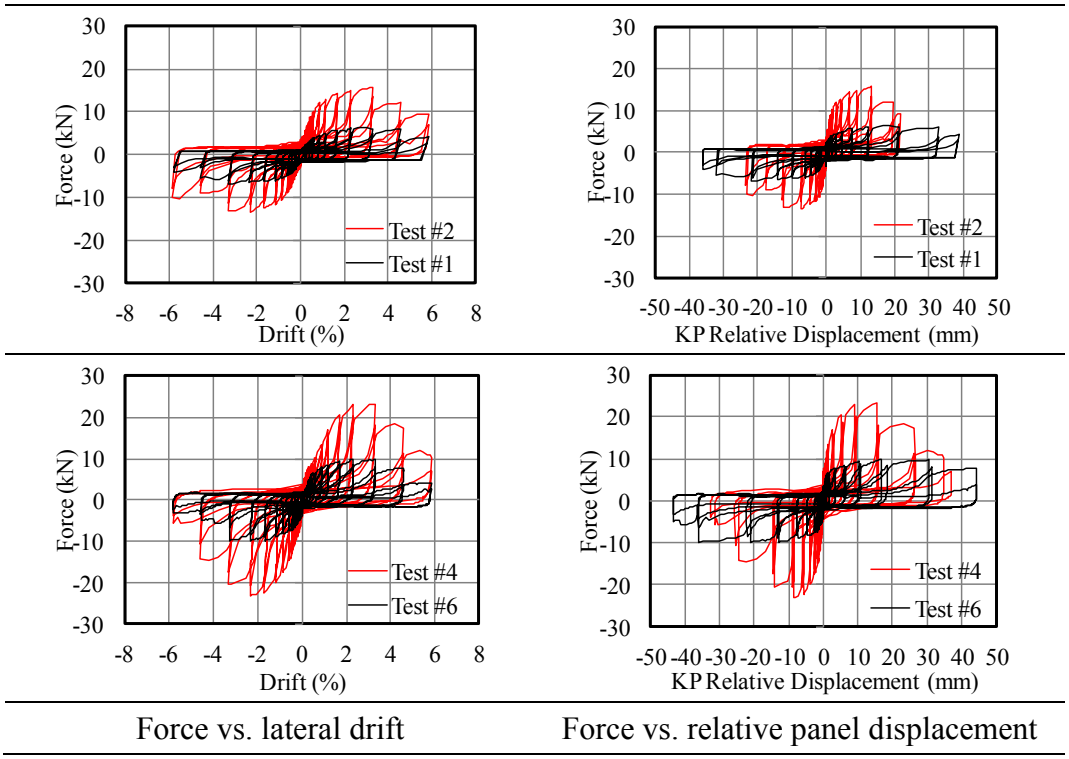

Fig. 13. Effect of fasteners on the cyclic behavior.

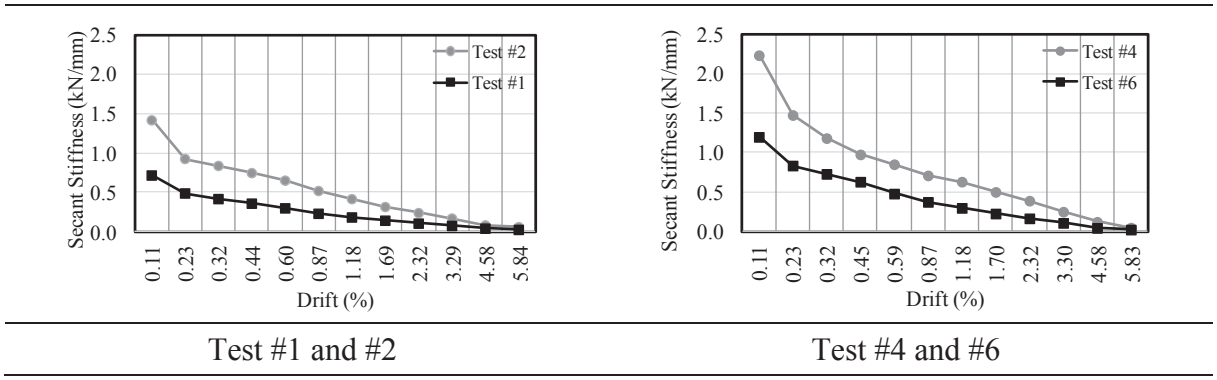

Fig. 14. Effect of fasteners on the secant stiffness.

affected from the loading direction. The specimens tested in parallel direction with the ribs yielded a higher strength and better global hysteretic behavior. It is similar to the behavior of parallel loaded mockup tests.

We compared the secant stiffness in Fig. 18. The specimens with ribs laid parallel to the loading direction gave higher stiffness values than the ones having ribs laid in the perpendicular direction.

A summary of the experimental results are tabulated in Table 9. The maximum strength was obtained in test #4 in which the loading was parallel to the ribs, and the improved fastener arrangement was used. The relative panel displacement was observed at 1% drift in tests #4 and #5.

Although the effect of the core foam density is not evaluated, an increase in the density may increase the initial stiffness because it increases the buckling capacity of the sandwich panels [3].

The in-plane roof stability cannot be supplied in the current form of construction practice (using one fastener at each crest). However, an increased number of fasteners will increase the load-carrying capacity of the sandwich panels. The increased capacity might be sufficient to use the sandwich panels instead of steel bracing units.

3. The analytical study

The analytical study consists of two portions associated with mockup and system tests. Primarily, an analytical equation was derived to estimate initial in-plane stiffness of the sandwich panels. The equation was then utilized to determine the results of the system tests.

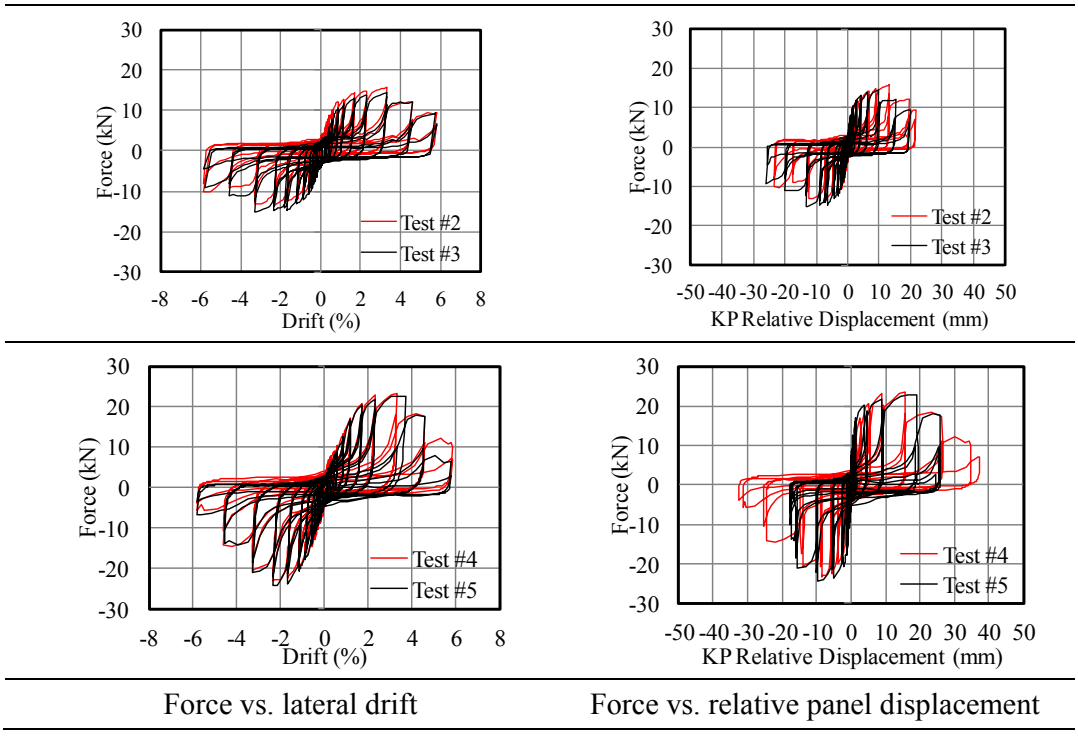

Fig 15. Effect of ribs on the cyclic behavior.

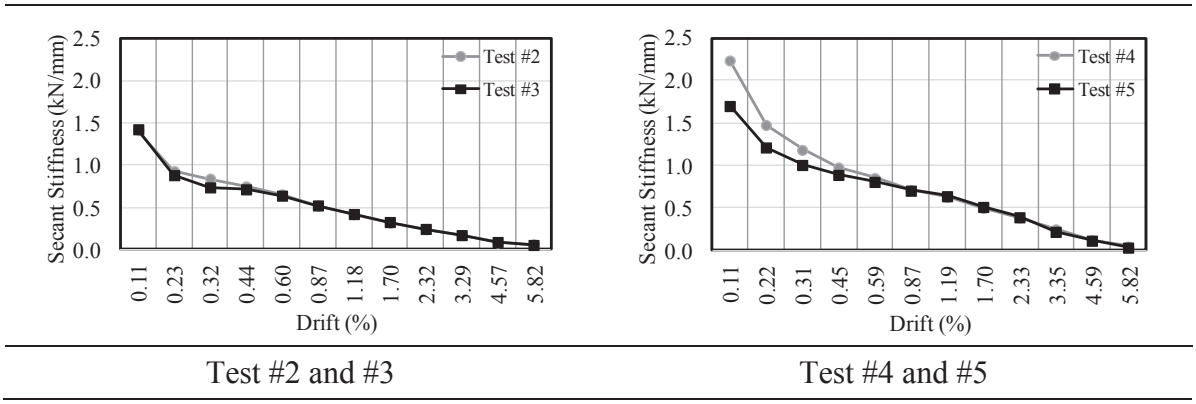

Fig. 16. Effect of ribs on the secant stiffness.

3.1. Tensile strength

Two discrete tensile capacities are defined to represent the possible collapse mechanisms of the panels. These are *sheet yielding around holes* (Fig. 19a) and *sheet yielding at body* (Fig. 19b). The first one is more realistic for practice. The second one represents an extreme case.

The force corresponding to sheet yielding around holes is calculated by Eq. (1a). Here, $\alpha$is the effective area factor for fasteners (~0.86), γ is direction factor, D is diameter of fastener, t_1 and $t_2$are sheet thicknesses, and f_y is the yield strength of the sheets. The total capacity of the panel (F_{ty}) is calculated by Eq. (1b) where n is the number of fasteners.

$$F_{hy} = \alpha \times \gamma \times \left(\pi \times \frac{D}{2}\right) \times (t_1 + t_2) \times f_y \tag{1a}$$

$$F_{ty} = n \times F_{hy} \tag{1b}$$

The direction factor of γ is suggested in Table 10. The suggestions are mainly based on the mockup test results.

The force corresponding to sheet yielding at body(F_{by})is calculated by Eq. (2) where w stands for the panel width.

$$F_{by} = w \times (t_1 + t_2) \times f_y \tag{2}$$

The experimental results of the mockups subjected to the parallel loading and their analytical estimations by Eq. (1b) are presented

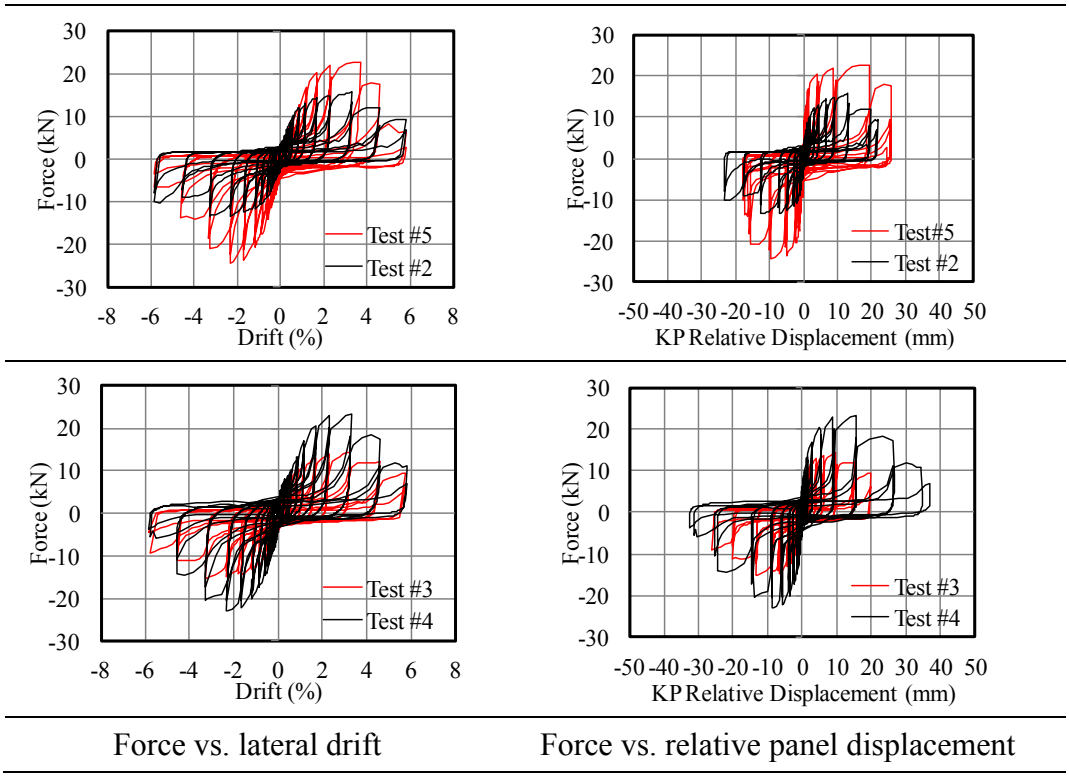

Fig. 17. Effect of loading direction on the cyclic behavior.

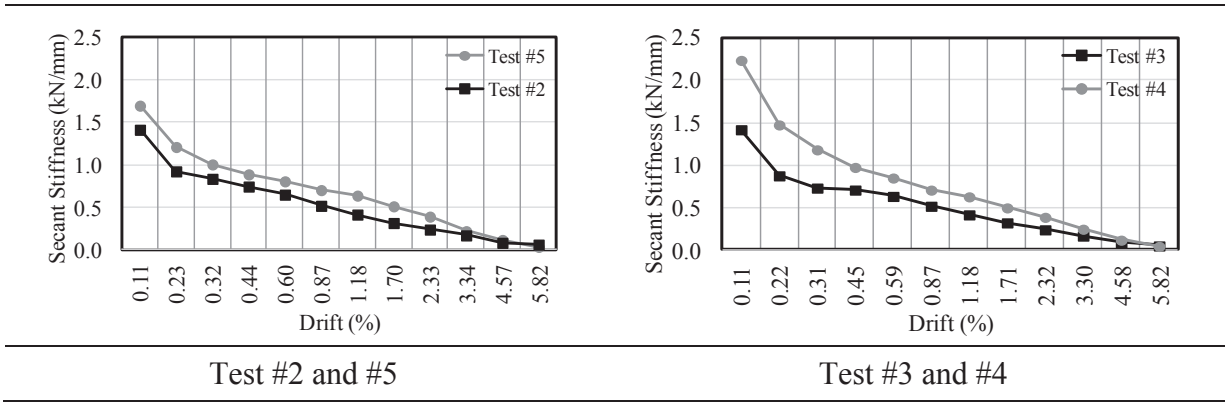

Fig. 18. Effect of the loading direction on the secant stiffness.

Table 9
Summary of system tests.

Test #	Max. strength (kN)	Drift@ max. strength (%)	Max. Drift (%)	Ultimate force @ max. drift (kN)	Initiation of relative vert. disp. (%)	Relative vertical displ.(mm) @ max. strength	Max. Relative displ. (mm)
1	6.20	2.32	5.84	4.24	0.31/0.44	12.22/7.14	38.70/23.20
2	15.74	3.29	5.84	9.36	0.44/0.59	13.16/8.08	21.80/16.18
3	14.42	3.29	5.78	9.34	0.44/0.59	9.88/7.36	19.88/15.58
4	23.30	3.31	5.82	6.99	0.87/1.18	15.62/9.02	37.10/19.54
5	22.65	3.49	5.80	6.55	0.87/1.18	19.20/9.50	25.84/13.78
6	9.97	2.32	5.83	3.89	0.59/0.59	16.92/17.58	44.22/48.46

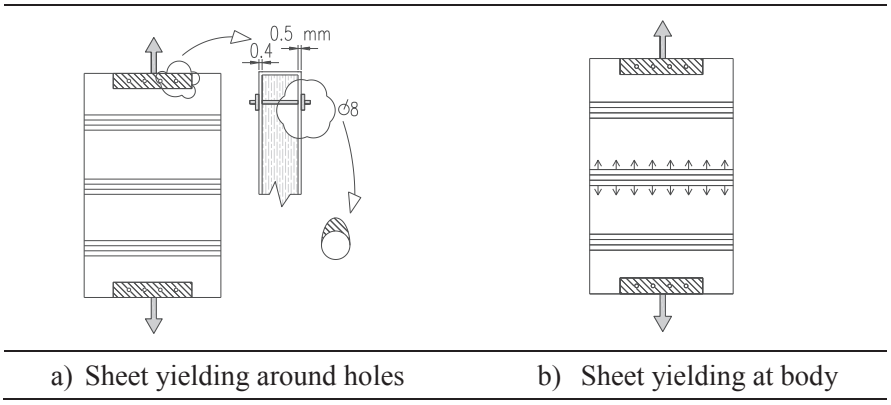

Fig. 19. Two damage modes for tensile loading.

Table 10
γ values.

Loading Direction	4 ribs	2 ribs
Parallel	1.00	1.00
Perpendicular	0.50	0.75

Table 11
Analytical evaluation of the specimens loaded in the parallel direction.

Exp. vs. Analy.	Yield Strength (kN)					
	Test#1	Test#2	Test#3	Test#4	Test#9	Test#10
Experimental	43.61	23.45	44.60	21.41	73.14	34.04
Analytical	41.36	20.68	41.36	20.68	69.45	34.72
Rel. Dif. (%)	5.16	11.81	7.26	9.68	5.05	2.00

together in Table 11. The results are in close agreement with each other.

The experimental results of the mockups subjected to the perpendicular loading and their analytical estimations by Eq. (1b) are presented together in Table 12. The results agree well with each other.

Since the damage accumulation mostly took place around the holes, the specimens were not reached to(F_{by})that was calculated as 241 and 455 kN for 0.9 and 1.7 mm total sheet thicknesses, respectively.

3.2. Effective initial in-plane stiffness

The stiffness properties of the sandwich panel systems vary via the increment of the displacement intensities. The initial and peak-to-peak (p-to-p) stiffness of the first cycles in *System Test #1* are exposed in Fig. 20a where the initial stiffness (k_i) is about 3.6 kN/mm and *peak-to-peak* stiffness is about 0.7 kN/mm. Tearing occurs around the fasteners once the displacement intensities increase. A typical cycle form is illustrated in Fig. 20b and could be observed throughout the test. A parallelogram is positioned in ±1% drift cycle by excluding the end regions (Fig. 20c). Peak-to-peak stiffness is calculated by connecting the corners of the parallelogram.

Force-displacement curves of the mockup tests and envelopes of force–displacement cycles of the system tests are accessible in Fig. 21a and b, respectively. A 1.0% drift ratio is allocated as "*representative yield limit*" for the specimens. This was exposed by blue dashed lines in the figures. This work is seen in that a 2% drift ratio was shown by dashed red lines and is a good indicator for the maximum loading capacity.

Table 12
Analytical evaluation of the specimens loaded in the perpendicular direction.

Exp. vs. Analy.	Yield Strength (kN)					
	Test#5	Test#6	Test#7	Test#8	Test#11	Test#12
γ	0.50	0.50	0.75	0.75	0.50	0.50
Experimental	18.19	10.80	31.70	17.91	33.43	21.60
Analytical	18.38	9.19	27.58	13.78	34.72	17.36
Rel. Dif. (%)	1.04	14.91	13.00	23.06	3.86	5.77

The *effective stiffness*($k_{0.01}$)corresponding to *representative yield limit* (1.0% drift ratio) could be calculated as ratio of total panel capacity(F_{ty}) to yield displacement of $0.01 \times L$ where L is span length of the sandwich panel Eq. (3).

$$k_{0.01} = \frac{F_{ty}}{0.01 \times L} \tag{3}$$

Eq. (3) can be rewritten as given in Eq. (4).

$$k_{0.01} = \frac{\alpha \times \gamma \times \left(\pi \times \frac{D}{2}\right) \times (t_1 + t_2) \times f_y \times n}{0.01 \times L} \tag{4}$$

3.3. Equivalent truss model

The behavior of the sandwich panels might be represented by 2D or 3D finite elements. However, the equivalent diagonal strut approach (1D) is preferred here due to its simplicity and efficiency in the preparation and analyses of the numerical model.

The pseudo elastic truss model consists of diagonal elements and is proposed for the representation of the effective in-plane stiffness and strength of the sandwich panels. The model will provide great simplicity to append the sandwich panels into the main structural model.

A unit of sandwich panel is represented by a couple of truss members. Axial stiffness(EA) of a truss member is calculated by Eq. (5) where $L_p$is length of the member.

$$EA = k_{0.01} \times L_p \tag{5}$$

The equivalent truss models were prepared for the system tests (Fig. 22). In the models, the hinged testing frame and the sandwich panels were represented by bold and thin lines, respectively.

Static analyses of the linear-elastic models were performed by *Seismo-Struct* software [22]. The variables used in the calculation of axial

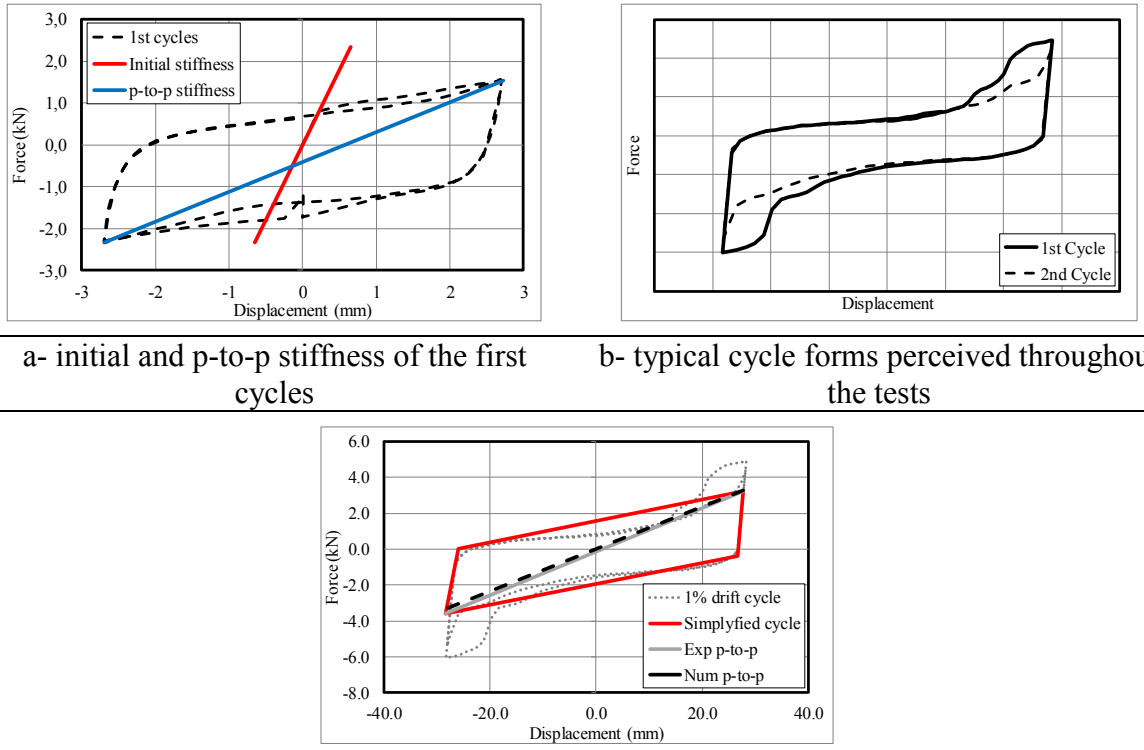

a- initial and p-to-p stiffness of the first cycles

b- typical cycle forms perceived throughout the tests

c- p-to-p stiffness for 1% drift level

Fig. 20. Stiffness definitions.

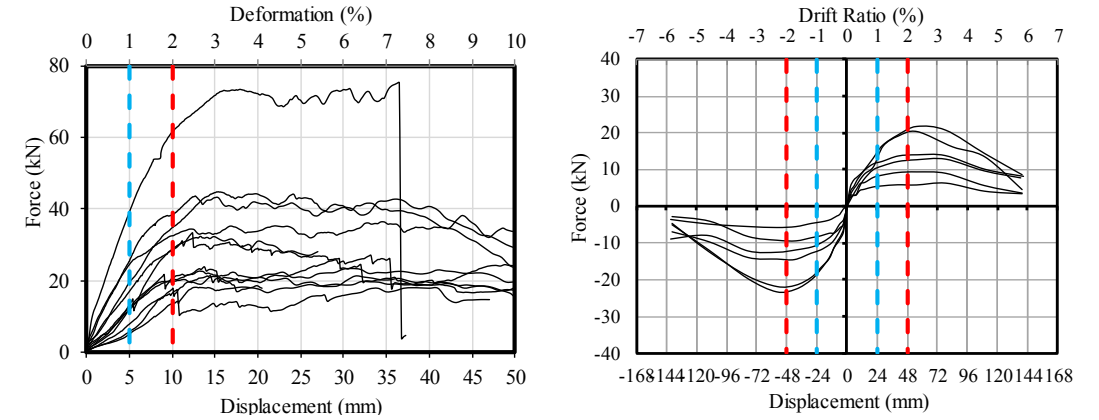

Mockup Tests *System Tests*

Fig. 21. Force-displacement relations obtained from the performed tests.

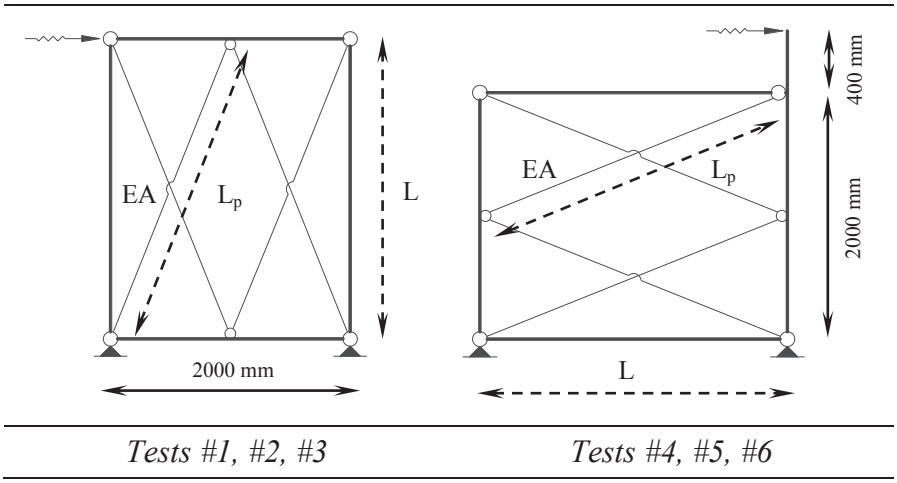

Fig. 22. Numerical modelling of the performed system tests.

Table 13
The variables used in calculation of axial stiffness of the truss members.

System Test #	D (mm)	n (pieces/m)	f_y (MPa)	$t_1 + t_2$ (mm)	L (mm)	γ	$k_{0.01}$ (N/mm)
1	4	2.5	255	0.9	2400	0.5	64.6
2	4	5.5	255	0.9	2400	0.5	142.1
3	4	5.5	255	0.9	2400	0.5	142.1
4	4	5.5	255	0.9	2400	1.0	284.2
5	4	5.5	255	0.9	2400	1.0	284.2
6	4	2.5	255	0.9	2400	1.0	129.2

stiffness of truss members are listed in Table 13.

The numerical results (blue dashed lines) were presented together with the experimental force–displacement cycles (Fig. 23).

Fig. 23 shows that the numerical assessments of *effective stiffness*($k_{0.01}$)and *maximum load bearing capacity* are successful enough. Relative differences between the numerical and experimental results are calculated in Table 14. The average relative differences were calculated as 11.78% and 10.63% for maximum strength and effective stiffness, respectively.

4. Conclusions

A comprehensive experimental research was conducted to comprehend in-plane shear behavior of corrugated sandwich panels and to propose the pseudo-elastic truss model. The conclusions could be derived as follows:

1. The experimental results show that the loading direction, sheet thickness, and number of fasteners are most effective parameters on the in-plane shear behavior of corrugated sandwich panels.
2. In the mockup tests, the modulus of elasticity was determined in the range of 50,000 to 240,000 MPa. The average value was calculated as 84,000 MPa. Poisson's ratio was obtained between 0.3 and 0.4 in the tests.
3. In the system tests, load–displacement hysteresis was greatly affected by tearing of thin sheet plates of corrugated sandwich panel. Hence, stiffness properties in cyclic loading could be better represented by a *three partite stiffness model.*
4. Tearing of thin sheet plates around the fasteners and rupture of fasteners were common damages observed in the system tests and could be deferred by using more fasteners on the overlapping of adjacent panels and crests.
5. The drift ratio of 2% is a critical value on which maximum strength is reached in all tests. Dependently, a 1% drift ratio was utilized in the determination of pseudoelastic stiffness.
6. Evaluation of the proposed equation for tensile capacity yields minimum and maximum differences of 1.04 and 23.06%, respectively. The average value is calculated as 8.55%.
7. The pseudoelastic truss model was evaluated in terms of effective stiffness and maximum strength in the system tests. The average differences between the estimated and experimental results are 11.78% and 10.64% for ultimate strength and effective stiffness, respectively.

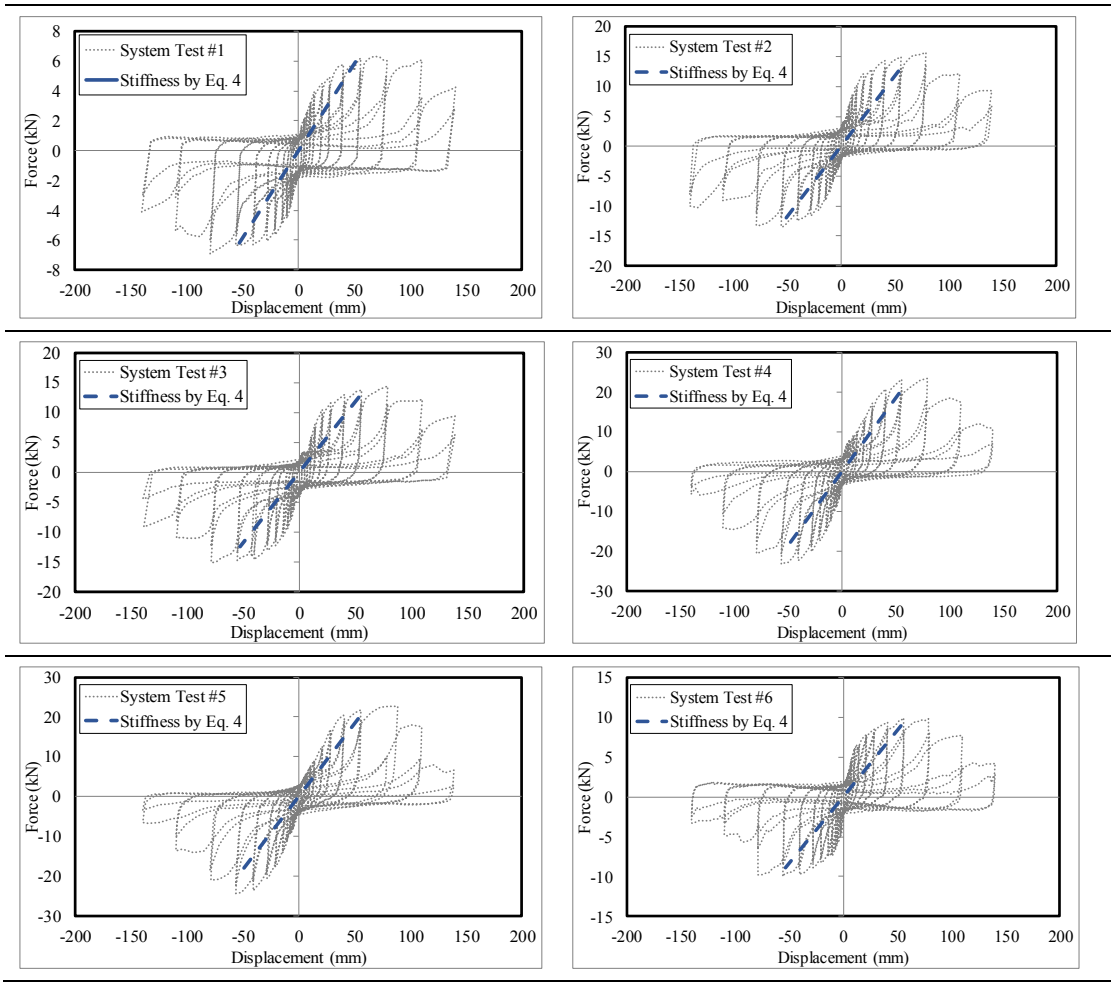

Fig. 23. The numerical estimations vs. experimental results.

Table 14
The comparison of experimental and numerical results.

System Test #	F_{max} (kN)			$k_{0.01}$ (kN/mm)		
	Exp.	Num.	Rel. Dif. (%)	Exp.	Num.	Rel. Dif. (%)
1	6.38	6.47	1.41	0.1172	0.1077	8.11
2	14.88	12.56	15.59	0.3053	0.2370	22.37
3	14.89	12.57	15.58	0.2668	0.2370	11.17
4	23.10	19.62	15.07	0.3211	0.3701	15.26
5	22.22	19.44	12.51	0.3701	0.3667	0.92
6	9.97	8.92	10.53	0.1790	0.1683	5.98
Average			11.78			10.64

Declaration of Competing Interest

The authors declare that they have no known competing financial interests or personal relationships that could have appeared to influence the work reported in this paper.

Acknowledgements

This study was conducted in the framework of İTÜNOVA Technology Transfer Office Research Project titled "*Determination of In-plane Behavior of Corrugated Sandwich Panel Type Roof Shelters.*" The financial support provided by Turkish Precast Concrete Association through this project is greatly appreciated. The study was conducted at the Structural and Earthquake Engineering Laboratory (STEELab) of Istanbul Technical University. Support of the laboratory staff and the contributions of Günkut Barka and Hakan Ataköy are gratefully acknowledged.

References

[1] Türkiye Bina Deprem Yönetmeliği, Afet ve Acil Durum Yönetimi Başkanlığı, Resmi Gazete, Sayı: 30364 (Mükerrer) 2018; in Turkish.
[2] European recommendations on the stabilization of steel structures by sandwich panels. International Council for Research and Innovation in Building and Construction, CIB Publication 379, 2013.
[3] Mahfuz H, Islam S, Saha M, Carlsson L, Jeelani S. Buckling of sandwich composites; effects of core-skin debonding and core density. Appl Compos Mater 2005;12:73–91.
[4] Dariushi S, Sadighi M. A study on flexural properties of sandwich structures with fiber/metal laminate face sheets. Appl Compos Mater 2013;20:839–55.
[5] Mostafa A, Shankar K, Morozov EV. Insight into the shear behavior of composite sandwich panels with foam core. Mater Des 2013;2013(50):92–101.
[6] Mostafa A, Shankar K, Morozov EV. Experimental, theoretical and numerical investigation of the flexural behaviour of the composite sandwich panels with PVC foam core. Appl Compos Mater 2014;21:661–75.
[7] Avci O, Luttrell LD, Mattingly J, Easterling WS. Diaphragm shear strength and stiffness of aluminum roof panel assemblies. J Thin Walled Struct 2016;106:51–60.
[8] Yu Y, Hou W, Hu P, Ying L, Akhmet G. Elastic constants for adhesively bonded corrugated core sandwich panels. Compos Struct 2017;176:449–59.
[9] Qi G, Ma L. Experimental investigation of composite pyramidal truss core sandwich panels with lightweight inserts. Compos Struct 2018;187:336–43.
[10] Sarvestani HY, Akbarzadeh AH, Niknam H, Hermenean K. 3D printed architected polymeric sandwich panels: energy absorption and structural performance. Compos Struct 2019;200:886–909.
[11] Daliri V, Zeinedini A. Flexural behavior of the composite sandwich panels with novel and regular corrugated cores. Appl Compos Mater 2019;26:963–82.

[12] De Matteis G, Landolfo R. Structural behavior of sandwich panel shear walls: an experimental analysis. Mater Struct 1999;32:331–41.
[13] Mahendran M, Subaaharan S. Shear strength of sandwich panel systems. Aust J Struct Eng 2002;3(3):115–26.
[14] Rogers CA, Tremblay R. Inelastic seismic response of frame fasteners for steel roof deck diaphragms. J Struct Eng 2003;129(12):1647–57.
[15] Essa HS, Tremblay R, Rogers CA. Behavior of roof deck diaphragms under quasi-static cyclic loading. J Struct Eng 2003;129(12):1658–66.
[16] Peirick L, Dawood M. In-plane shear behavior of full-scale structural GFRP sandwich panels for building applications. Proceedings of the 6th International Conference on FRP Composites in Civil Engineering. 2012.
[17] Massarelli R, Edward Franquet J, Shrestha K, Tremblay R, Rogers CA. Seismic testing and retrofit of steel deck roof diaphragms for building structures. J Thin Walled Struct 2012;61:239–47.
[18] Hamid NHA, Fudzee MF. Seismic performance of insulated sandwich wall panel (ISWP) under in-plane lateral cyclic loading. Int J Emerg Technol Adv Eng 2013;3:1–7.
[19] Choi KB, Choi WC, Feo L, Jang SJ, Yun HD. In-plane shear behavior of insulated precast concrete sandwich panels reinforced with corrugated GFRP shear connectors. Compos B Eng 2015;79:419–29.
[20] Motamedi M, Ventura CE. Inelastic response of steel roof deck diaphragms with nailed and welded connections. Eng Struct 2016;117:10–25.
[21] Saghayesh AM. In-plane behaivour of sandwich panels. M.Sc. Thesis, Istanbul Technical University Graduate School of Science Engineering and Technology, June 2017.
[22] SeismoStruct, Computer program for static and dynamic nonlinear analysis of framed structures. http://www.seismosoft.com.